ADVANCED MATERIALS

# Supporting Information

for *Adv. Mater.*, DOI: 10.1002/adma.201801347

# From Wood to Textiles: Top-Down Assembly of Aligned Cellulose Nanofibers

*Chao Jia, Chaoji Chen, Yudi Kuang, Kun Fu, Yilin Wang, Yonggang Yao, Spencer Kronthal, Emily Hitz, Jianwei Song, Fujun Xu, Boyang Liu, and Liangbing Hu**

# Supporting Information

**From Wood to Textiles: Top-down Assembling Aligned Cellulose Nanofibers**

*Chao Jia, Chaoji Chen, Yudi Kuang, Kun Fu, Yilin Wang, Yonggang Yao, Spencer Kronthal, Emily Hitz, Jianwei Song, Fujun Xu, Boyang Liu, and Liangbing Hu**

*Characterizations*: The microstructures of the natural wood, delignified wood and wood-textile fibers were determined by a field emission scanning electron microscopy (FESEM, HITACHI SU-70). The FTIR spectra of the natural wood and delignified wood were measured using a Fourier transform infrared (FTIR) spectroscopy system (Thermo Nicolet NEXUS 670) in the range of 650~4000 $cm^{-1}$ wavenumber. Small angle X-ray scattering (SAXS) measurement was made using a Xenocs Xeuss 2.0 SAXS system. The mechanical properties of the samples were determined using a tensile tester (Tinius Olsen H5KT). The resilience percentage of the fibers was determined using a universal tensile testing machine (WDW-100E) at two different conditions. One used a constant elongation of 5%, and another used a constant stress of 3 N. The preset stress for all resilience measurements was set as 1 N. X-ray diffraction patterns of the wood samples were measured using an XRD system (Rigaku RAPID II, Rigaku Americas Corp) equipped with Cu Kα radiation in the 2θ range of 5~80°. The conductivity was measured by a four-point collinear probe method. A Keithley 2400 SourceMeter was used to supply a current between the two farthest electrodes, and a Keithley 2182A Nanovoltmeter was used to measure a voltage between the two intermediate electrodes. The structure durability against water and mechanical stirring was determined by magnetically stirring the wood-textile fibers in a beaker with DI water at a speed of 150-700 rpm.


**Figure S1.** Delignified wood film. After delignification, the yellowish color of the natural wood was removed and the white color was obtained.

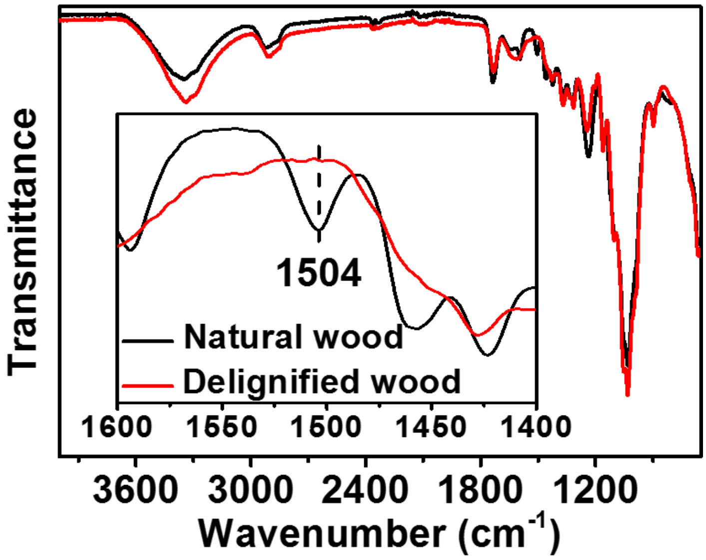


**Figure S2.** FTIR spectra of the natural wood and delignified wood. The complete removal of lignin in delignified wood can be confirmed from the absence of aromatic skeletal vibration peak of benzene ring at 1504 $cm^{-1}$.

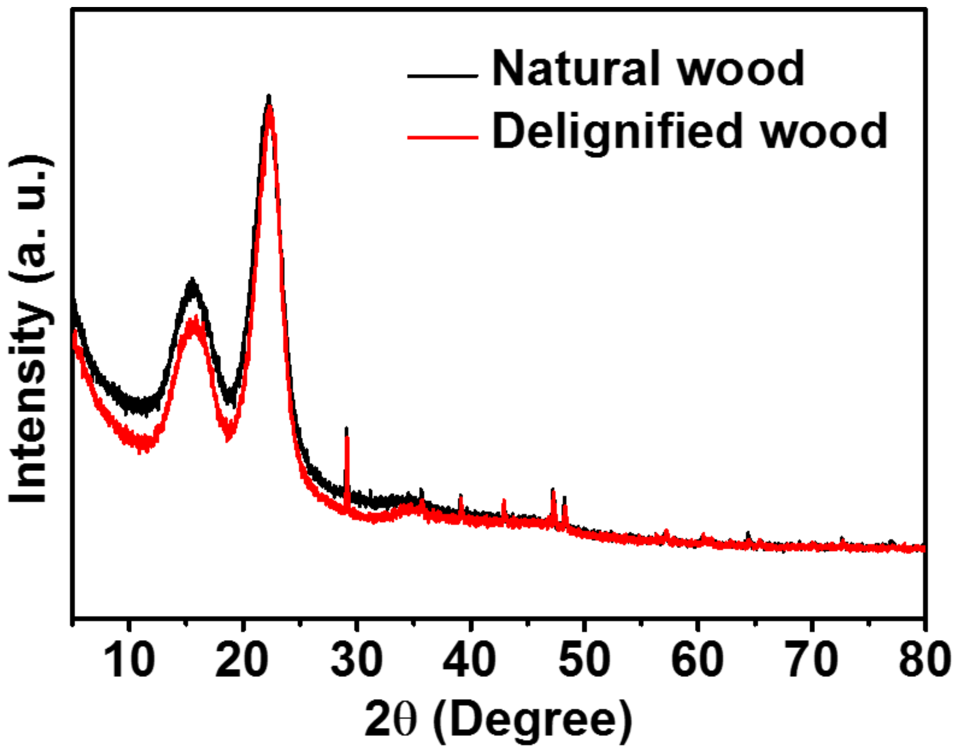


**Figure S3.** XRD patterns of the natural wood and delignified wood. The delignification process does not significantly change the cellulose crystal structure.

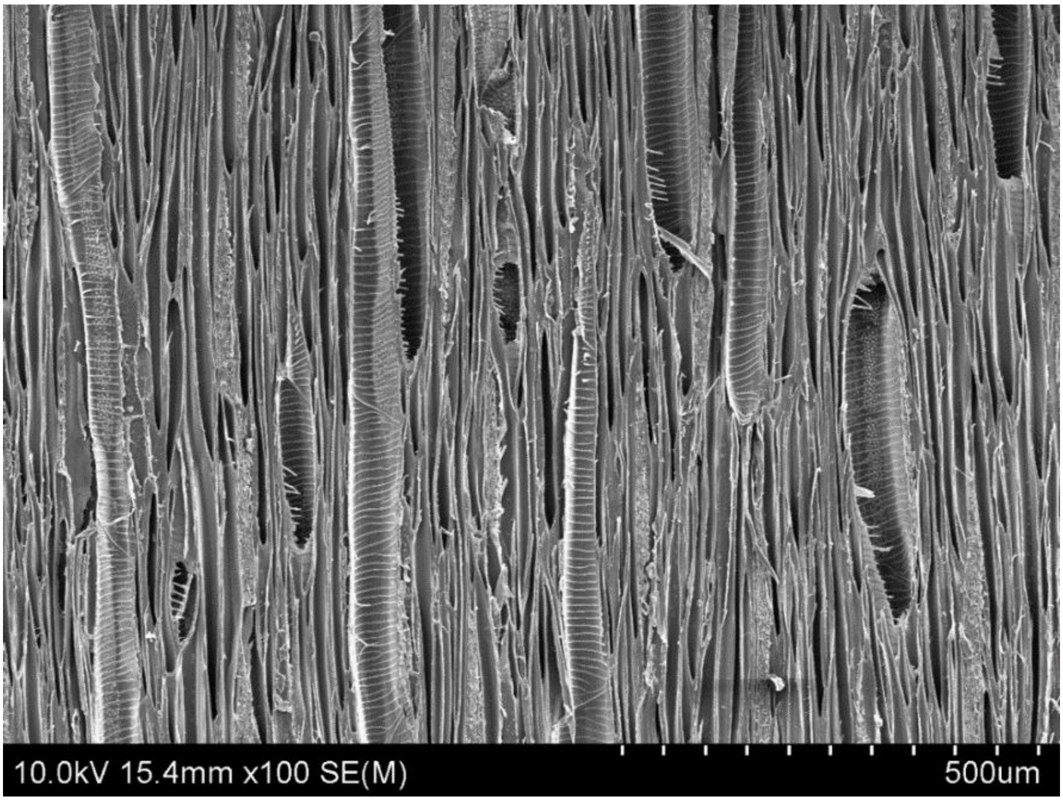


**Figure S4.** Vertically aligned microchannels, which are the main paths for the transport of water, ions, and other nutrients in trees, can be visualized in the natural wood.

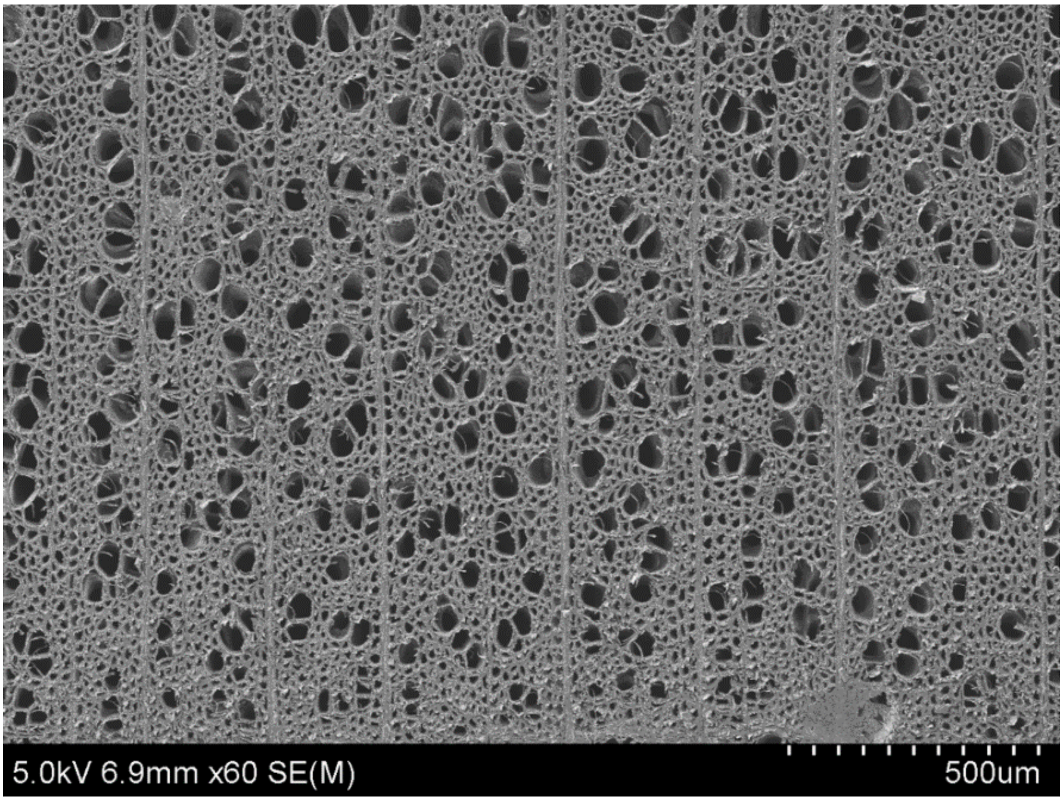

**Figure S5.** Top-view SEM image of natural wood. The uneven and well-defined pore structures can be clearly observed.

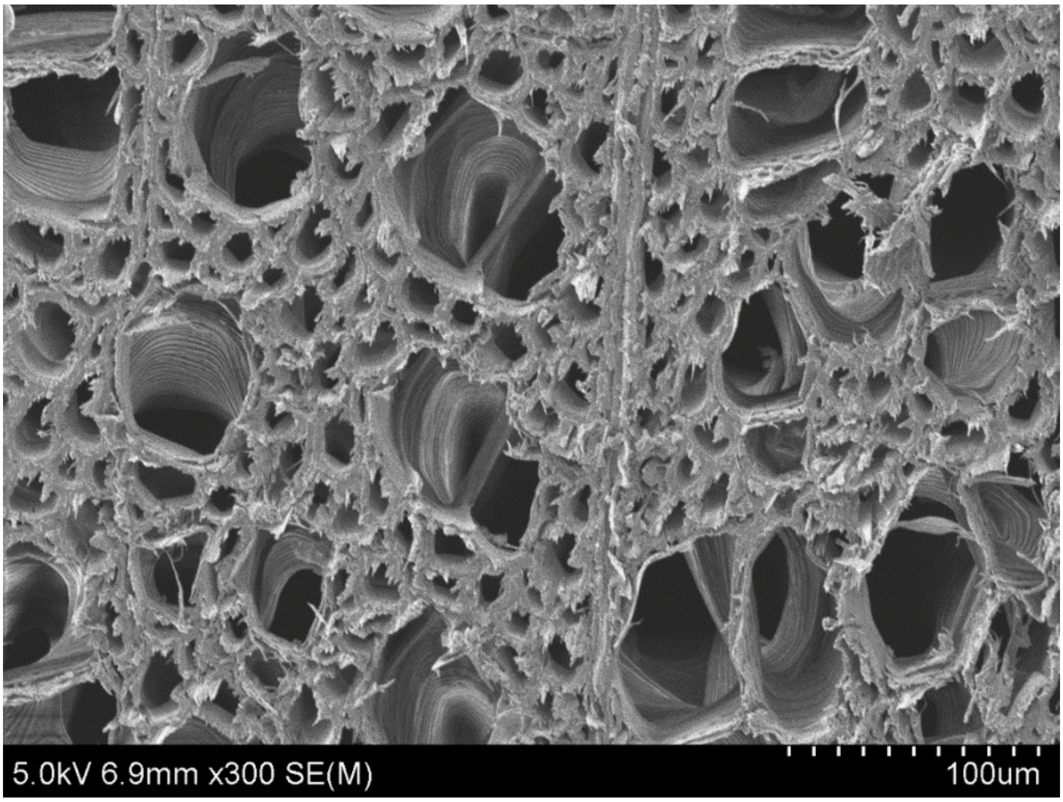


**Figure S6.** Top-view SEM image of natural wood. The uneven and well-defined pore structures can be clearly observed.

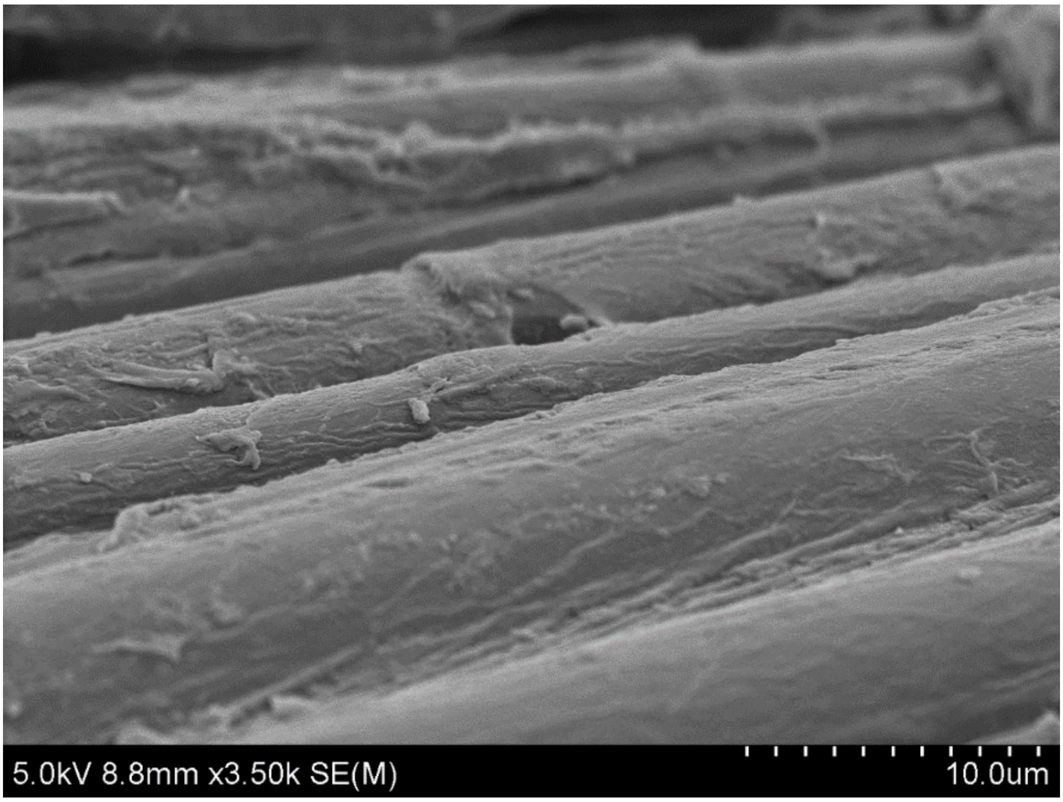


**Figure S7.** High-magnification SEM image of the wood-textile fiber lateral surface to show the collapsed aligned microchannels.

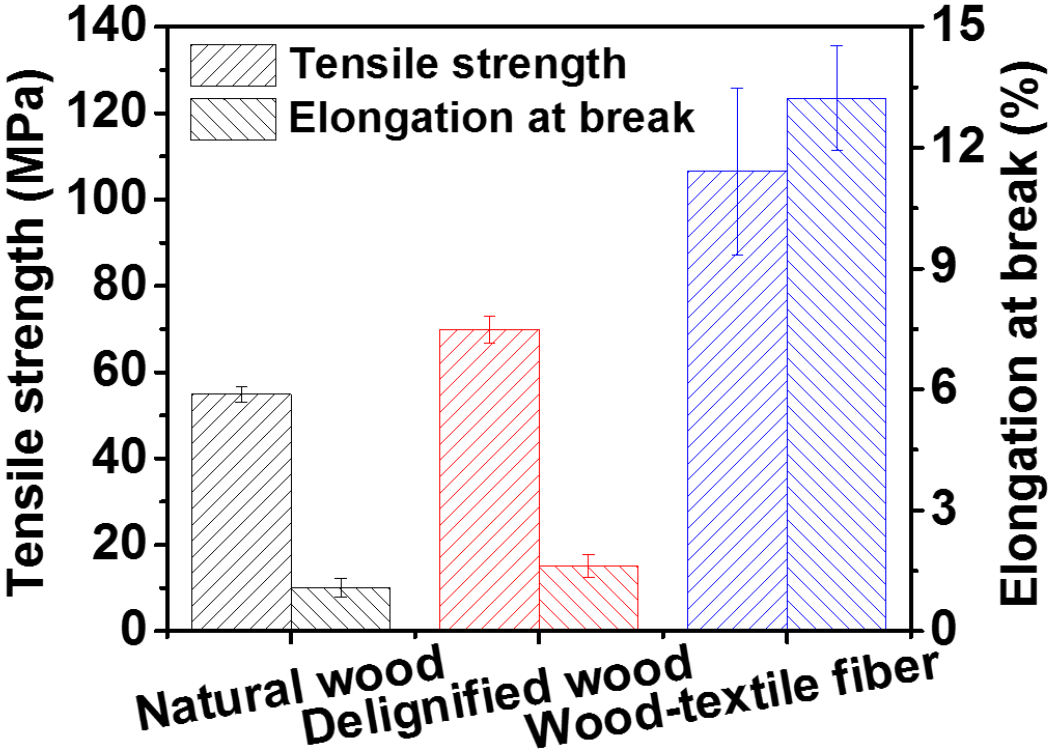


**Figure S8.** Tensile strength and elongation at break of natural wood, delignified wood, and wood-textile fiber.

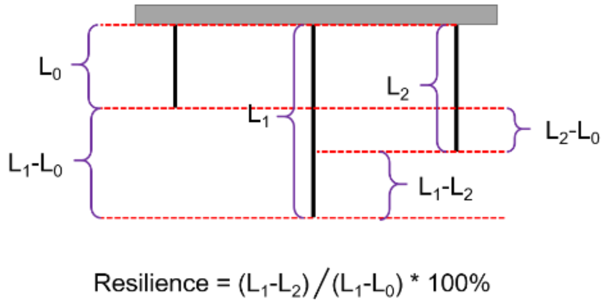


**Figure S9.** Graphical illustration of the determination of resilience.

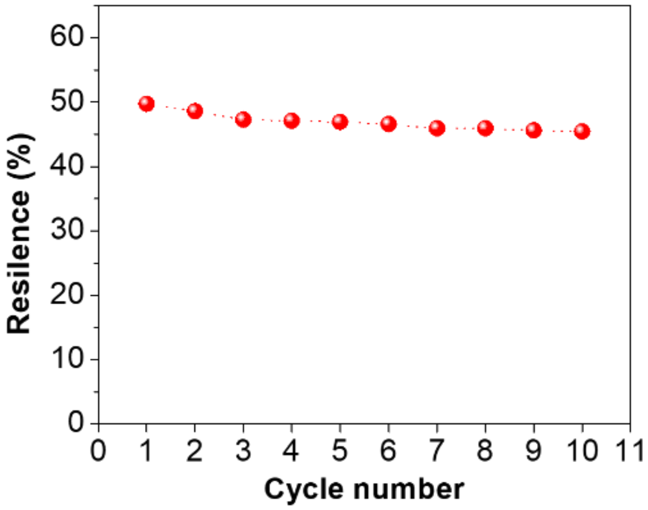


**Figure S10.** Resilience of the wood-textile fiber at different cycle numbers measured with constant strain.

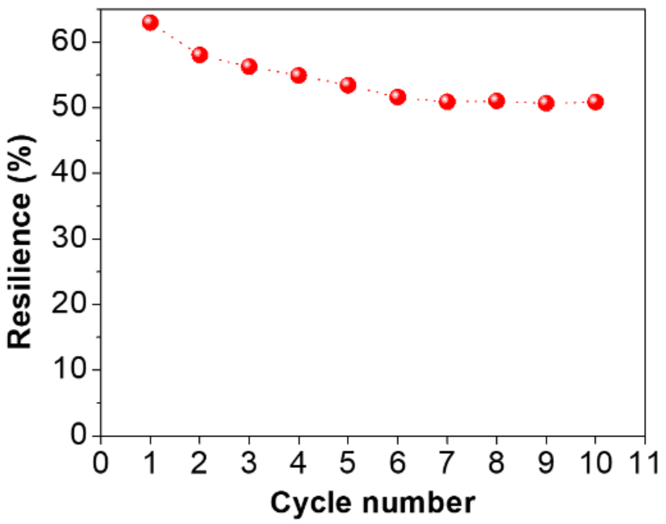


**Figure S11.** Resilience of the wood-textile fiber at different cycle numbers measured with constant stress.

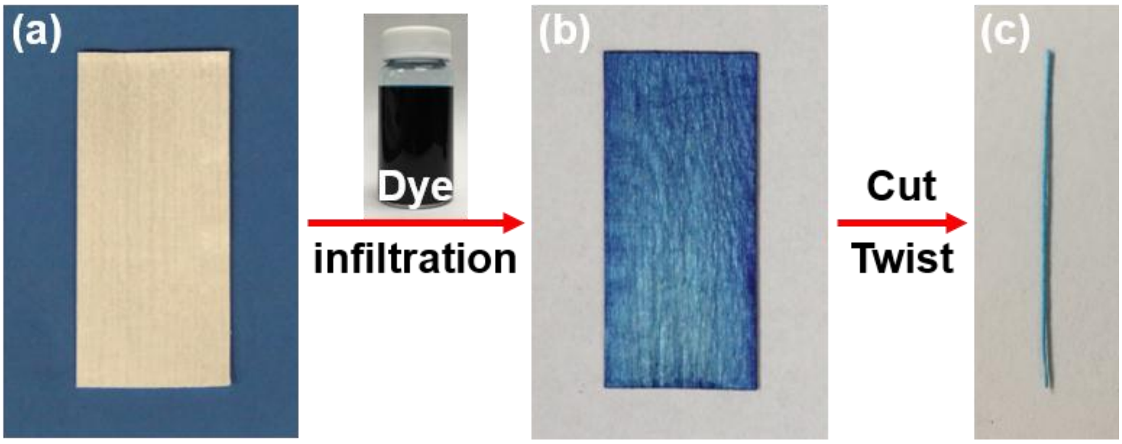


**Figure S12.** (a) Digital image of a delignified wood film. (b) Digital image of a delignified wood film infiltrated with methylene blue. (c) Digital image of a dyed wood-textile fiber prepared by cutting and twisting the dyed wood film.

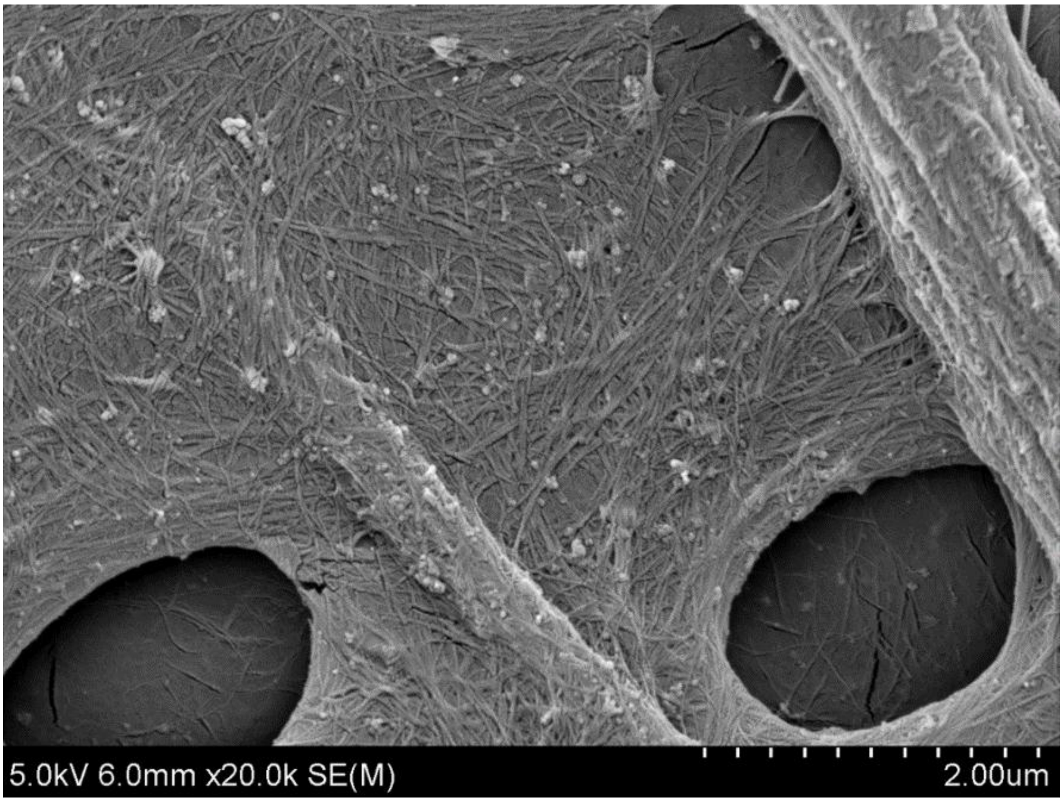


**Figure S13.** SEM image of the infiltrated CNTs in the microchannels of the delignified wood.

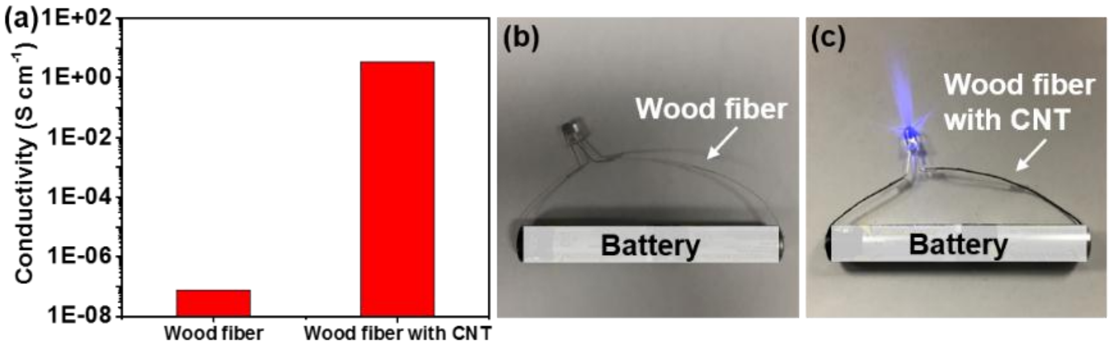


**Figure S14.** (a) Electrical conductivity of wood fiber and wood fiber loaded with CNTs. (b) Digital image to demonstrate the wood fiber without CNTs cannot be used as wire to light up a LED bulb. (c) Digital image to demonstrate the wood fiber loaded with CNTs can be used as wire to light up a LED bulb.

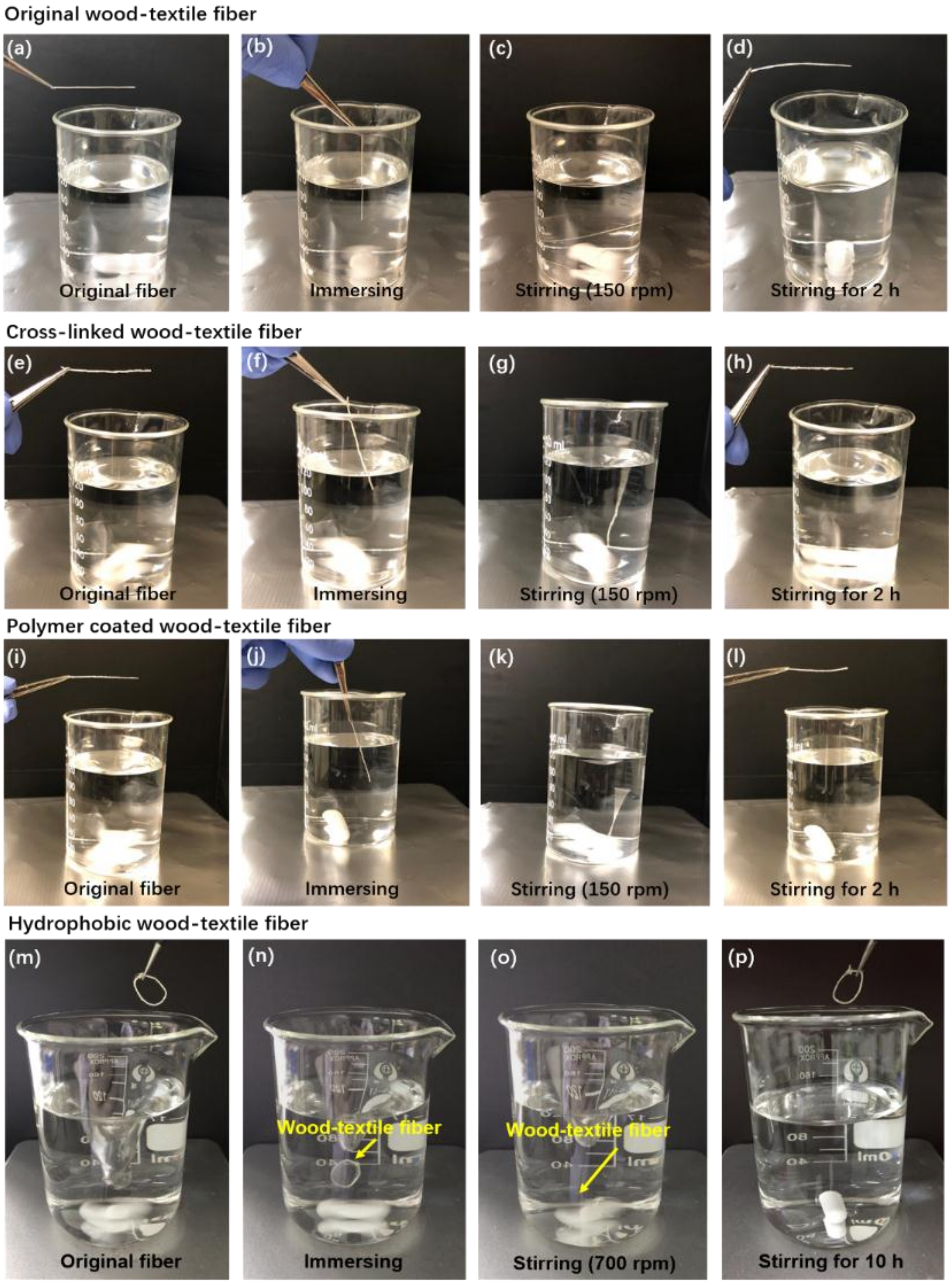


**Figure S15**. Digital images to show the structure durability against water and mechanical stirring of various wood-textile fibers: (a-d) original wood-textile fiber, (e-h) cross-linked wood-textile fiber, (i-l) polymer coated wood-textile fiber, and (m-p) hydrophobic wood-textile fiber.